Aust. Met. Mag. 38 (1990) 99–106

Fog formation at Perth Airport

Huang Xinmei*, T.J. Lyons and R.O. Pitts
Environmental Sciences, School of Biological and Environmental Sciences, Murdoch University, Western Australia

(Manuscript received May 1989; revised March 1990)

A modified numerical mesoscale model, neglecting the microphysics of condensation, is developed to predict fog formation and validated against detailed case studies. When initialised with routinely available airport observations, simulations illustrate an ability to predict fog formation in the vicinity of Perth Airport. Although requiring saturation to indicate fog formation, these studies illustrate the potential of a simplified version for routine fog forecasting.

Introduction

Fog forms in the lower atmosphere when the air becomes saturated, provided that sufficient condensation nuclei are available. This may occur by either cooling the air to its dew-point or through the addition of moisture, raising the dew-point to equal the temperature. The formation of radiation fog is primarily dominated by a balance between radiative cooling and turbulence (Turton and Brown 1987; Gerber 1981). For example, Davis (1957) observed that on a calm and clear night the air temperature fell rapidly by radiative cooling, whilst eddy diffusion shaped the humidity profile and resulted in a dew-point inversion in the lower layers of air. A thin layer of fog first formed at the layer of maximum water vapour concentration. Roach et al. (1976) also found that fog formed with a lull in wind speed. They noted that the radiative cooling rate deduced from radiative flux divergence measurements was greater than the actual cooling rate, and suggested that radiative cooling encourages fog formation whereas turbulence inhibits it.

Brown and Roach (1976), using a one-dimensional model, argued that turbulence hinders the formation of fog, as the smaller their exchange coefficient was, the earlier radiation fog formed. However, Gerber (1981) argued that fog formation is caused by turbulent mixing of nearly saturated eddies.

Comparing his observations to the models used by Brown and Roach (1976) and Roach (1976) without the incorporation of turbulence, he showed that fog formed rapidly and water vapour supersaturation values were an order of magnitude larger than predicted by the models. Gerber (1981) suggested both effects were attributable to turbulence. Analysing their observations, Lala et al. (1982) found that increased wind and hence turbulent mixing may promote or prevent fog formation. Welch et al. (1986), applying a number of turbulent exchange methods in their model, noted that the loss of energy by turbulent transport is more important than radiative cooling during fog formation. They suggested that increased turbulence led to radiation fog formation.

Studies of radiation fog carried out in England have been reviewed by Mason (1982). He concluded that fog formation is determined by favourable synoptic systems and local factors like turbulence and radiative cooling. The observations showed that fog commonly forms more or less over areas of a few hundred square kilometres. This implies that the vertical structure of atmosphere mainly determines fog formation, whilst mesoscale flow or the effects of local terrain are at least partly responsible.

Fog formation aloft has been observed by some authors, suggesting that other factors besides turbulence and radiation are involved. Pilie et al. (1975) found that deep valley fog first formed slightly below the point of maximum cooling rate in the air at about 100 m. They suggested that this was caused by a mountain wind cooling the middle and lower layers of the air. Meyer et al. (1986) argued that fog may be actually formed in an elevated layer or elsewhere and advected over the field site by local flows.

* Permanent affiliation: Department of Meteorology, Beijing Institute of Meteorology, People's Republic of China.

Other kinds of fogs, such as advection fog, have not been studied in as much detail. Barker (1977) developed a two-dimensional maritime boundary model to predict and study the effect of meteorological changes on the formation and dissipation of fog. The numerical experiments showed that the energy budget is an important process in advection fog. The location of fog formation is highly sensitive to the moisture content upstream, while changes in wind speed have less effect at the fog location.

An operational numerical model for the prediction of fog has been described by Karlsson and Falk (1984). It is based on a one-dimensional model and considers advection by moving a column of air along a mean trajectory in the boundary layer. They simulated the influence of terrain by assuming that air temperature changes adiabatically with the terrain height. Although their simulations were in general agreement with observations, the results were found to be more dependant on boundary conditions than initial meteorological profiles.

As the prediction of fog formation is of fundamental importance for aviation, and detailed observations of temperature, humidity and wind in the boundary layer are often not routinely available, this paper presents a preliminary analysis of the use of a numerical mesoscale model to predict fog formation in the vicinity of Perth Airport.

Climate

Perth, Western Australia, is located at approximately 32°S, 116°E, on the relatively featureless Swan coastal plain, terminated to the east by the 300 m high Darling Scarp, about 20 km from the coast. This escarpment, which descends to plain in 3–5 km, marks the western edge of an inland plateau and stretches for approximately 200 km in a north/south direction. The major airports in the vicinity are located to the west of the Darling Scarp with Perth Airport, Guildford, lying approximately 7 km from the escarpment (Fig. 1).

The climate is characteristically Mediterranean with mild wet winters and hot dry summers. Storms and frontal systems originating over the Indian Ocean during winter bring moisture inland. Fogs generally occur from March to October and are more frequent between May and August (Gentilli 1971).

Analysis of fogs observed at Perth Airport during the year July 1987 to July 1988, showed that they can be subdivided into four types; radiation fog, post-frontal fog, advection fog and rain fog. Radiation fog occurs under light synoptic pressure gradients when there are light winds and clear skies, whereas post-frontal fog is found when a front is followed by a high pressure system or ridge. Frontal precipitation increases the availability of moisture during the day and radiative cooling at night results in fog formation. If the front is not strong, the effect of advection may be negligible. Advection assists fog formation through either moisture advection, increasing water vapour in the lower air, or thermal advection when cold air passes over a moist surface. Rain fog occurs when rain falling through a layer of cooler air near the ground evaporates, saturating the cold air near the surface. Most rain fogs form on overcast nights after the rain stops and therefore, radiative cooling is small. Of the thirteen nights of fog observed during 1987–88, six were classified as rain fog, three as advection and two each as radiation and post-frontal fog. The predominance of rain fog has also been noted elsewhere (Liu 1987).

Fig. 1 Perth region, showing location of major airports and significant topographical features.

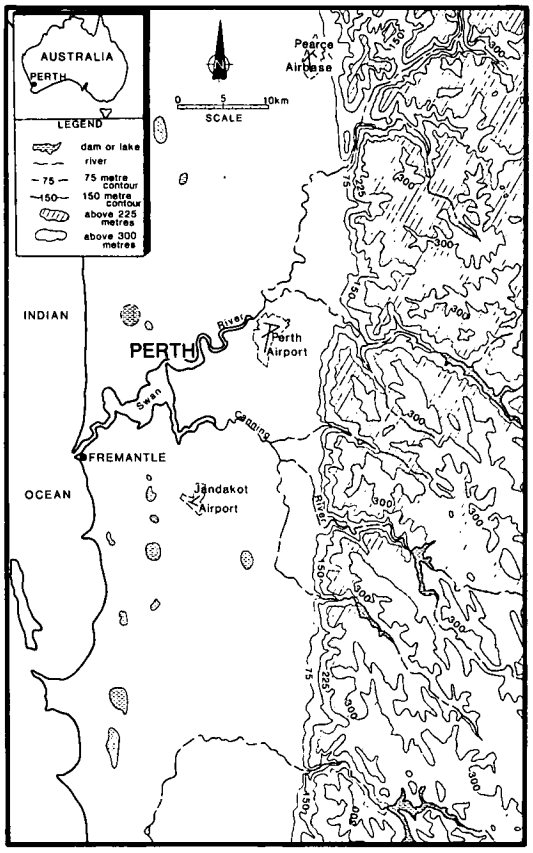

Model

The numerical mesoscale model is based on that described by McNider and Pielke (1981), with modifications in the boundary layer parametrisation and incorporation of condensation and

liquid water. In particular, since we are only interested in fog formation rather than its development, the temperature, water vapour and liquid water distributions were estimated from the following continuity equations (Brown and Roach 1976):

$$\partial T/\partial t = -(1/\rho c_p)\,\partial F_n/\partial z + \partial/\partial z(K_h \partial\theta/\partial z) + LC/c_p$$
$$\partial q/\partial t = \partial/\partial z(K_q \partial q/\partial z) - C$$
$$\partial w/\partial t = \partial/\partial z(K_w \partial w/\partial z) + \partial G/\partial z + C$$

where T is the dry-bulb temperature, θ the potential temperature, ρ density, c_p the specific heat of air at constant pressure, F_n the net radiative flux, K_h, K_q, K_w exchange coefficients for heat, water vapour and liquid water respectively, L latent heat of vaporisation, C rate of condensation per unit mass of air, q humidity mixing ratio, w liquid water mixing ratio, and G gravitational settling flux of liquid water.

Within the model subgrid-scale fluxes are parametrised by an eddy exchange coefficient. For the convective boundary layer, McNider and Pielke (1981) described the eddy diffusion coefficients by a cubic polynomial formulation (O'Brien 1970) whereas under stable conditions they replaced this by a local scheme (Blackadar 1979). Given the importance of turbulence in the formation of fog, this was replaced by a scheme derived from the turbulent kinetic energy (TKE) equation following Yamada (1983) and Arritt (1985). It was further assumed that $K_h = K_q = K_w$ and the height of the boundary layer was defined as the first height above the surface where the TKE $< 10^{-3}$ m^2 s^{-2} (Arritt 1985).

The model does not allow for supersaturated conditions and does not calculate the growth of fog droplets. Rather it is assumed that if the air is supersaturated, water is condensed and latent heat released to the air. Liquid water in an unsaturated environment is evaporated and latent heat absorbed from the air. Brown (1980) has shown that the difference in predicted time of fog formation between a drop growth scheme and the saturation adjustment method used here is not large.

The gravitational settling flux of liquid water was represented as

$$G = 0.0625w^2$$

which implies a similar drop spectrum to that observed in the United Kingdom at Cardington, characterised by large concentrations of small droplets (Brown and Roach 1976). Dew deposition was calculated from surface energy balance depending on the sign of the latent heat flux, F_l (Severin et al. 1984). For $F_l > 0$, dew deposition was assumed whereas for $F_l < 0$, evapotranspiration took place. The rate of dew deposition, r_w, was defined as F_l/L, where L is the latent heat of vaporisation. As the surface specific humidity, q(0), cannot exceed the surface saturated specific humidity, $q_s(0)$ (Deardorff 1978), the surface wetness, f_p, is set to unity for dew deposition in estimating the surface specific humidity from

$$q(0) = f_p q_s(0) + (1-f_p)q(1)$$

where q(1) is the specific humidity at first vertical grid (Turton and Brown 1987). At other times f_p is specified using the concept of surface resistance (Monteith 1981) and given by

$$f_p = (z_2/K_{h1})/(z_2/K_{h1} + r_s)$$

where K_{h1} is the exchange coefficient for the bottom layer, z_2 the height of the first grid-point above the surface, and r_s, the surface resistance, has been arbitrarily taken as 60 s m^{-1} (Turton and Brown 1987; De Bruin and Holtslag 1982). This yields typical values of 0.7 for f_p and accounts for actual evaporation being less than the potential evaporation which occurs over a saturated surface.

The long wave flux is modified by the presence of liquid water in the atmosphere and hence the effective emissivity of a water cloud (Stephens 1978) has been adopted for the liquid water in the fog. The upward, E_u, and downward, E_d, emissivity of liquid water are given as

$$E_{wl} = E_d = 1 - \exp(-0.158u_w)$$
$$E_{wl} = E_u = 1 - \exp(-0.13u_w)$$

where u_w is the liquid water path in g m^{-2}. For water vapour, Rodgers' (1967) emissivity function has been used. Assuming the equality of absorbtivity and emissivity, and that the individual transmittances are multiplicative (Paltridge and Platt 1976), leads to a transmittance of

$$(1-E) = (1-E_{wv})\,(1-E_{co2})\,(1-E_{wl})$$

where E_{wv}, E_{co2} are the emissivities for water vapour and carbon dioxide respectively (Garratt and Brost 1982). Downward long wave radiation is taken to be zero at the tropopause.

Since we are not interested in the dispersal of fog by solar radiation and turbulent mixing, standard formulations for solar radiation on a horizontal surface under clear skies were adopted. As well, typical values of atmospheric transmission for Western Australia were used (Lyons and Edwards 1982) and no allowance was made for scattering by fog droplets.

Validation

The model was validated by simulating the radiation fog case studies of Turton and Brown (1987). In this the model was initialised with their initial profiles of temperature, specific humidity and soil temperature. As well, their modified solar radiation equation was adopted to yield optimum agreement with the measured hourly mean values of the downward short wave flux (Turton and Brown 1987).

The observed and modelled surface energy fluxes are shown in Fig. 2 for their case study A. Turton and Brown (1987) estimated the observed sensible heat flux as a residual from the other fluxes and hence this component also contains the residual errors associated with the measurements. Predicted energy budget components are in close agreement with the observations, especially the long wave and soil heat fluxes.

Fig. 2 Observed and modelled surface energy fluxes for case study A (Turton and Brown 1987).

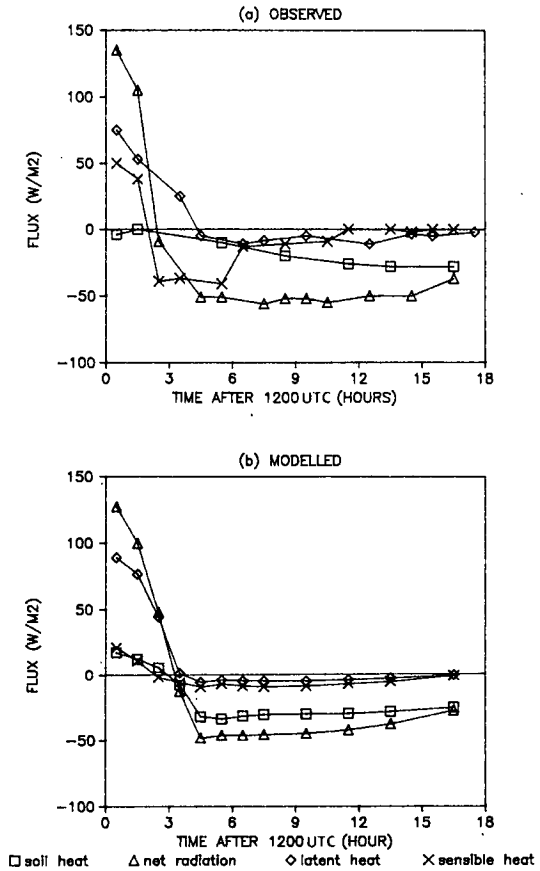

Figure 3 illustrates the predicted and observed profiles of temperature, specific humidity and wind speed at 2300 h. The profiles of temperature and specific humidity are similar to the observations, with a well defined surface-based inversion. Wind speeds are slightly higher in the lower air.

Fig. 3 Predicted and observed profiles of temperature, specific humidity and wind speed at 2300 h for case study A (Turton and Brown 1987).

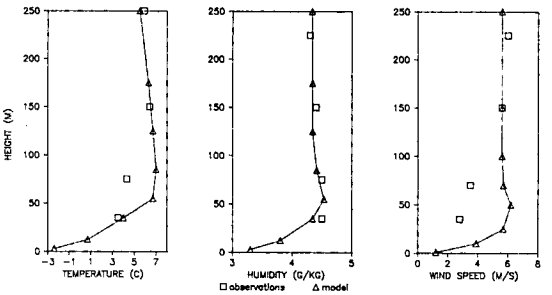

Turton and Brown (1987) reported the formation of mist between 2000 and 0600 h. Within the model, the onset of surface-based fog was observed at 0100 h, and the fog developed slowly upwards reaching a height of 35 m by 0800 h. Of course the model equates fog formation with a relative humidity of 100 per cent and we are unable to distinguish between mist and fog. Figure 4 shows the predicted and observed temperature and relative humidity trends at 1 and 35 m. The higher observed temperature after midnight and early morning is caused by advection of warmer, drier air in the boundary layer (Turton and Brown 1987) which has not been accounted for in our model, which assumes a constant geostrophic wind. Nevertheless, the results are in reasonable agreement with the observations before 0100 h at 35 m although the 1 m temperature is slightly lower.

Fig. 4 Predicted and observed temperature and relative humidity trends at 1 and 35 m for case study A (Turton and Brown 1987).

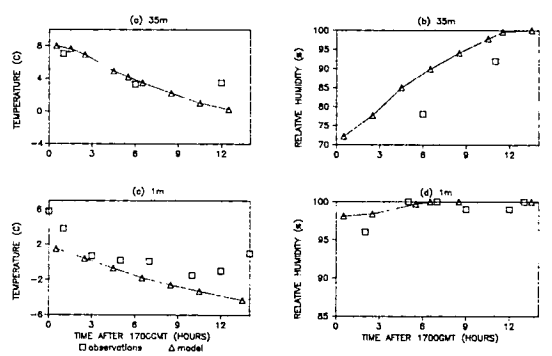

Figure 5 shows the predicted and observed screen level temperature and relative humidity as well as wind speed at 10 m as a function of time for their case study B. In this case the model produced a higher wind speed, while both the predicted temperature and relative humidity show good agreement with the observations after sunset. Fog was observed at 1730 h whilst the model predicted its formation at 1630 h.

In both of these simulations the model assumed a constant geostrophic wind, as specified by the synoptic pressure gradient, and assumed fog formation when saturation occurred.

Fig. 5 Predicted 3 m temperature, relative humidity and 10 m wind speed compared to screen observations and 10 m wind speed for case study B (Turton and Brown 1987).

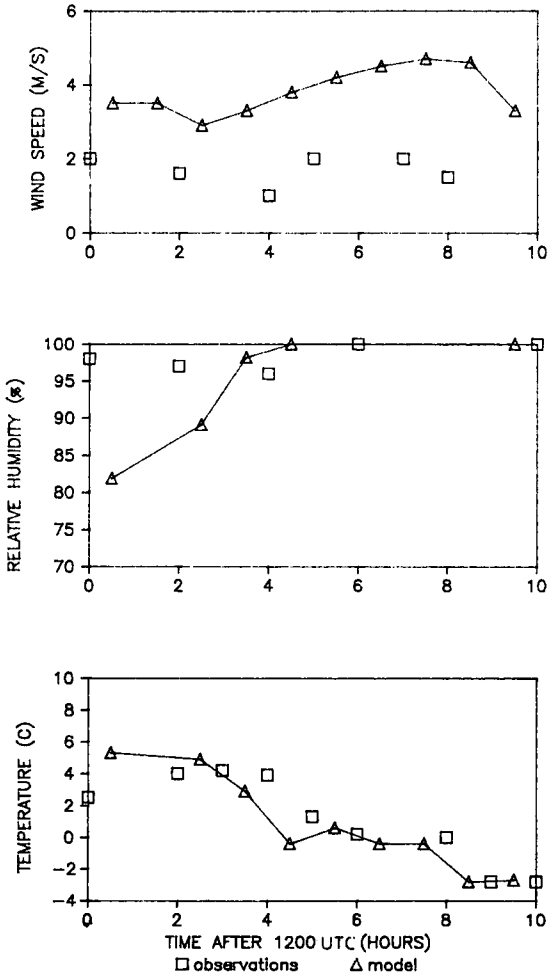

Perth experiments

Validation against the experiments of Turton and Brown (1987) relied on detailed observations for both model initialisation and comparison. However, in using the model for fog prediction at Perth Airport, only routine observations are available. Thus the model has been initialised with the 1100 UTC (1900 WST, local time) radiosonde profile.

The model soil heat flux and surface temperature are sensitive to the soil properties chosen. As no detailed thermal classification of Perth soils has been undertaken, values appropriate to a mixture of dry sandy soil and light soil with root have been used (Pielke 1984). Slightly different values are adopted for wet soil after the passage of rain and these are listed in Table 1, along with the constants used to initialise the model. An effective emissivity of 0.95 has been assumed for the ground.

Table 1. Soil thermal properties (after Pielke 1984).

	Specific heat capacity ($cal\ g^{-1}\ K^{-1}$)	*Density* ($g\ cm^{-3}$)	*Diffusivity* ($cm^2\ s^{-1}$)
Dry	0.30	1.3	0.0080
Wet	0.34	1.4	0.0074

At night, over the typically dry sandy soils of Perth, the latent heat flux is a small part of surface energy balance and the model was simplified by assigning a constant value of 0.15 to f_p. This is more representative of typical soil wetness in the vicinity of the airport and compatible to a value of 0.05 used elsewhere (Mahrer and Pielke 1977; Diab and Garstang 1984) for dry sandy soils. After dew deposition the soil wetness is set to 1.0.

The model has been run against the majority of fog days for 1987–88 and representative case studies for a radiation fog and a rain fog are presented. A typical radiation fog occurred on 24 October 1987 when the synoptic situation was characterised by a ridge of high pressure across the southwest of Western Australia producing a weak pressure gradient and a surface gradient wind of 5 m s^{-1} from 170° at Perth. Fog was reported at the airport between 0545 and 0630 WST.

As the synoptic system remained stable throughout the night, the model assumed a constant geostrophic wind speed and both one and two-dimensional versions were used with the appropriate dry soil parameters (Table 1). The flat one-dimensional model does not predict the occurrence of fog although the relative humidity reaches 98 per cent, whereas the two-dimensional

model, incorporating a smoothed terrain across the escarpment, forecasts the onset of fog at 0130 WST (Fig. 6). It should be noted that this model requires a relative humidity of 100 per cent for both fog formation and persistence, whereas Pruppacher and Klett (1978) have summarised a large collection of relative humidity measurements taken in fogs which suggest that the majority of maritime and continental fogs are unsaturated. Gerber (1981) suggests such fogs are unactivated fog containing only haze droplets whereas activated fog, requiring 100 per cent relative humidity, must contain some fog droplets. As shown in Fig. 6, the observed relative humidity, estimated from the dry and wet-bulb temperature readings, was below 100 per cent when fog was observed.

Table 2. Model parameters.

Vertical grid	1,2,4,8,12,20,30,40,60,80, 120,160,220,300,400,600, 900,1400,2000 metres and the tropopause
Horizontal grid spacing	2-D model (40) 3 km
Time step	1-D model 60 s 2-D model 30 s

Fig. 6 Predicted temperature and relative humidity at 1.5 m for the 1 and 2-D models for October 24 compared to observations.

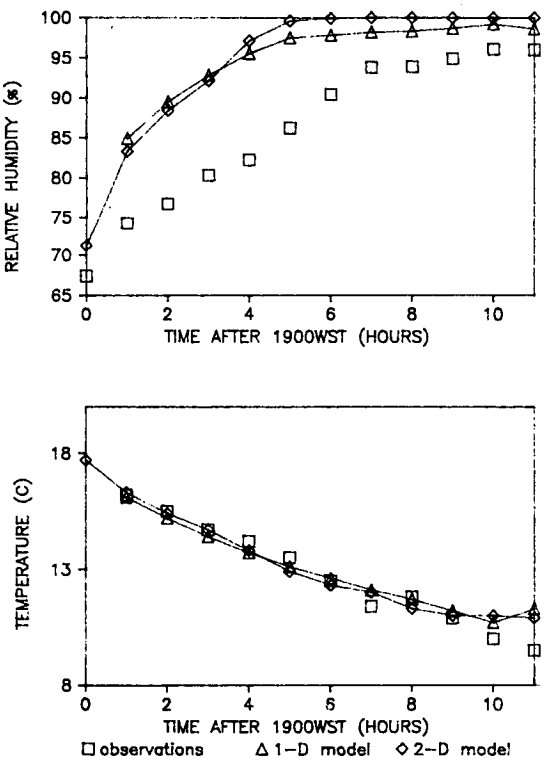

The one-dimensional model approaches saturation near the surface but never quite reaches it as moisture is removed from the air through dew deposition. Within the model, ground surface temperature is estimated from closure of the surface energy budget, and the surface specific humidity is maintained at or less than the equivalent saturation specific humidity based on this temperature. Given this continual depletion of vapour at the surface, turbulent mixing ensures that the relative humidity only approximates saturation. In the two-dimensional case, additional advection of colder air and the formation of fog in the immediate vicinity of the escarpment is sufficient to provide the marginal difference required for the prediction of fog at the airport location.

Figure 6 also highlights the predicted temperature at 1.5 m for both models compared to the observations. Although there is no significant difference between the models, the temperature drops slightly more quickly after midnight with the introduction of topography.

As the temperature structure is determined by both turbulent mixing and long wave flux divergence as well as advective cooling, Fig. 7 illustrates the model partitioning of these processes. In both cases the radiative cooling is very similar, whereas the introduction of topography leads to marked cooling centred on 50 metres above the surface. In the one-dimensional model, with cooling centred at the surface, the model formulation forces the moisture to be deposited out as dew, thus preventing fog formation. With the introduction of topography, maximum cooling occurs away from the surface sink for moisture, allowing the formation of fog.

Fig. 7 Computed profiles of the partitioning of the turbulent, radiative and advective (2-D model only) contributions to local warming for 2400 WST on 24 October. Warming rates are one-hour averages ending at the specified hour.

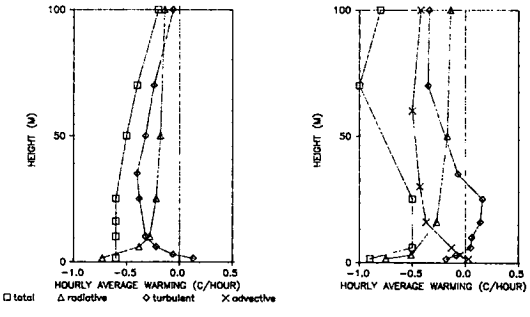

Figure 7 also illustrates that in this case the turbulence is acting to cool the air by mixing cold air up from the ground. Should the wind speed increase such that the enhanced mechanical mixing distributed heat more uniformly throughout the profile, then the turbulence would eliminate the fog by mixing warm air down from aloft.

A characteristic example of rain fog occurred on 26 May 1988 when a high pressure system ridged across the southwest of Western Australia following the passage of a weak cold front. It rained at 1800 WST and the sky above Perth was characterised by an average cloud cover of 0.7 made up of stratus or stratocumulus clouds. A weak synoptic pressure gradient led to a surface gradient wind of 6 m s^{-1} from 210° across the region. Fog was observed to form at Perth Airport at 2249 WST.

Fig. 8 Predicted temperature and relative humidity at 1.5 m for the 1-D model for May 26 compared to observations.

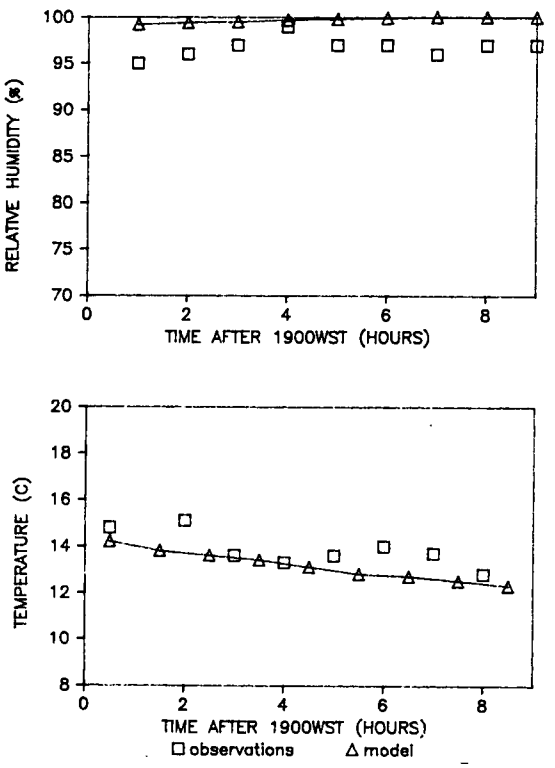

Although the rain had stopped, the cloud remained and hence needed to be accounted for in the radiation parametrisation of the model. However, with only the radiosonde profile available, it is not possible to ascertain the liquid water content of the cloud. As rain fog mainly results from increased moisture at the surface, the effect of the cloud is only considered on the surface radiation budget and the emissivity of liquid water is not computed. The long wave radiation at surface, R_l, is given by

$$R_l = R_c + cN$$

where R_c is long wave radiation at the surface for clear skies, N is the fraction of cloud cover and c was taken as 60 W m^{-2} (Paltridge and Platt 1976).

Since rain fog tends to occur under existing conditions of high relative humidity after rain and not be associated with strong radiative cooling, the one-dimensional model was used and the moist soil parameters assumed. This predicted that the air would become saturated aloft at an elevation of 35 m by 2230 WST and that the fog would spread downward by gravitational settling and turbulent mixing to the surface by 0030 WST. Both predicted and observed temperatures at 1.5 m are in close agreement (Fig. 8).

The partitioning between radiative and turbulent cooling, shown in Fig. 9, illustrates that the maximum rate of cooling occurred aloft. Thus turbulent mixing of this near-saturated air assisted in the initial formation of fog away from the moisture sink of dew deposition at the surface.

Fig. 9 Computed profiles of the partitioning of the turbulent and radiative contributions to local warming for 2200 WST on 26 May. Warming rates are one-hour averages ending at the specified hour.

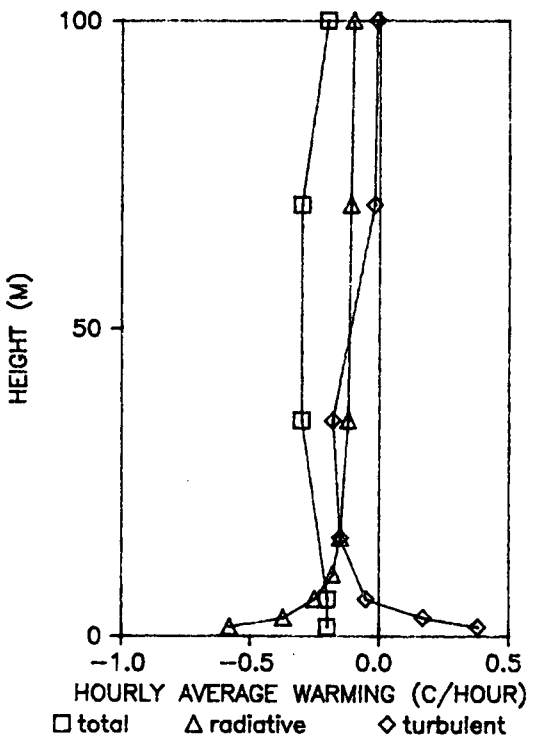

Conclusions

A modified numerical mesoscale model, neglecting the microphysics of condensation, has been validated against the detailed case studies of Turton and Brown (1987). When initialised with routinely available airport observations, simulations illustrate an ability to predict fog formation in the vicinity of Perth Airport. Although the simplified model requires saturation to indicate fog formation, these studies illustrate the potential of a one-dimensional version of the numerical mesoscale model for routine fog forecasting.

Acknowledgments

This work has been enhanced by the continued cooperation and encouragement of the Perth Regional Office of the Australian Bureau of Meteorology and, in particular, the staff of the Perth Airport office. Throughout it, Huang Xinmei was supported by the Government of the People's Republic of China, and R.O. Pitts was in receipt of a Commonwealth Postgraduate Award. All of this assistance is gratefully acknowledged.

References

Arritt, R.W. 1985. *Numerical studies of thermally and mechanically forced circulations over complex terrain.* Cooperative Institute for Research in the Atmosphere, Colorado State University, Fort Collins, Colorado 80523, USA, 201 pp.

Barker, E.H. 1977. A maritime boundary layer model for the prediction of fog. *Bound. Lay. Met., 11,* 267–94.

Blackadar, A.K. 1979. High resolution models in the planetary boundary layer. *Advances in Environmental and Scientific Engineering,* Vol. 1, Gordon and Breach, 50–85.

Brown, R. 1980. A numerical study of radiation fog with an explicit formulation of the microphysics. *Q. Jl R. met. Soc., 106,* 781–802.

Brown, R. and Roach, W.T. 1976. The physics of radiation fog. II: A numerical study. *Q. Jl R. met. Soc., 102,* 333–54.

Davis, F.K. 1957. Study of time height variation of micrometeorology factors during radiation fog. Part I: The physical processes in the formation of radiation fog. *Publication in Climatology, Vol. X, No. 1,* Drexel Institute of Technology Laboratory of Climatology, 1–37.

Deardorff, J.W. 1978. Efficient prediction of ground surface temperature and moisture, with inclusion of a layer of vegetation. *J. geophys. Res., 83,* 1889–903.

De Bruin, H.A.R. and Holtslag, A.A.M. 1982. A simple parameterization of the surface fluxes of sensible and latent heat during daytime compared with the Penman-Monteith concept. *Jnl appl. Met., 21,* 1610–21.

Diab, R.B. and Garstang, M. 1984. Assessment of wind power potential for two contrasting coastlines of South Africa using a numerical model. *Jnl Clim. appl. Met., 23,* 1645–59.

Garratt, J.R. and Brost, R.A. 1981. Radiative cooling effects within and above the nocturnal boundary layer. *J. Atmos. Sci., 38,* 2730–45.

Gerber, H.E. 1981. Microstructure of a radiation fog. *J. Atmos. Sci., 38,* 454–8.

Gentilli, J. (ed.) 1971. *Climates of Australia and New Zealand,* Vol. 13, World Survey of Climatology, Elsevier, Amsterdam, 405 pp.

Karlsson, E. and Falk, J.E. 1984. An operational numerical model for prediction of fog and stratus. *Proc. Nowcasting II Symposium,* Norrkoping, 1984, ESA SP-208, 335–40.

Lala, G.G., Jiusto, J.E., Meyer, M.B. and Kornfein, M. 1982. Mechanisms of radiation fog formation on four consecutive nights. *Preprints Conf. Cloud Physics,* Chicago, Amer. Meteor. Soc., 9–11.

Liu, H.F. 1985. Analysis and forecast of fog formation at Sun Shan and Taoyuan. (In Chinese, English summary.) *Meteorological Bulletin, 31,* 174–90.

Lyons, T.J. and Edwards, P.R. 1982. Estimating global solar irradiance for Western Australia, Part 1. *Arch. Met. Geophys. Bioklim., B, 30,* 357–69.

McNider, R.T. and Pielke, R.A. 1981. Diurnal boundary-layer development over sloping terrain. *J. Atmos. Sci., 38,* 2198–212.

Mahrer, Y. and Pielke, R.A. 1977. A numerical study of the airflow over irregular terrain. *Beitr. Phys. Atmos., 50,* 98–113.

Mason, J. 1982. The physics of radiation fog. *J. met. Soc. Japan, 60,* 486–98.

Meyer, M.B., Lala, G.G. and Jiusto, J.E. 1986. Fog 82: A cooperative field study of radiation fog. *Bull. Am. met. Soc., 67,* 825–32.

Monteith, J.L. 1981. Evaporation and surface temperature. *Q. Jl R. met. Soc., 107,* 1–27.

O'Brien, J.J. 1970. A note on the vertical structure of the eddy exchange coefficient in the planetary boundary layer. *J. Atmos. Sci., 27,* 1213–15.

Paltridge, G.W. and Platt, C.M.R. 1976. *Radiative processes in meteorology and climatology.* Elsevier, Amsterdam, 318 pp.

Pielke, R.A. 1984. *Mesoscale Meteorological Modelling.* Academic Press, New York, 612 pp.

Pilie, R.J., Mack, E.J., Komond, W.C., Rogers, C.W. and Eddie, W.J. 1975. The life cycle of valley fog. Part I: Micrometeorological characteristics. *Jnl appl. Met., 14,* 347–63.

Pruppacher, H.R. and Klett, J.D. 1978. *Microphysics of clouds and precipitation.* Riedel, Amsterdam, 714 pp.

Roach, W.T. 1976. On the effect of radiative exchange on the growth by condensation of a cloud or fog droplet. *Q. Jl R. met. Soc., 102,* 361–72.

Roach, W.T., Brown, R., Caughey, S.T., Garland, J.A. and Readings, C.J. 1976. The physics of radiation fog. Part I: A field Study. *Q. Jl R. met. Soc., 102,* 313–33.

Rodgers, C.D. 1967. The use of emissivity in atmospheric radiation calculations. *Q. Jl R. met. Soc., 93,* 43–54.

Severini, M., Moriconi, M.L. and Tonna, G. 1984. Dewfall and evapotranspiration determination during day- and nighttime on an irrigated lawn. *Jnl Clim. appl. Met., 23,* 1241–6.

Stephens, G.L. 1978. Radiation profile in extended water clouds. II: parameterization schemes. *J. Atmos. Sci., 35,* 2123–32.

Turton, J.D. and Brown, R. 1987. A comparison of numerical model of radiation fog with detailed observations. *Q. Jl R. met. Soc., 113,* 37–54.

Welch, R.M., Ravichandran, M.G. and Cox, S.K. 1986. Prediction of quasi-periodic oscillation in radiation fogs. Part I: Comparison of similarity approaches. *J. Atmos. Sci., 43,* 633–51.

Yamada, T. 1983. Simulations of nocturnal drainage flows by a q^2l turbulence closure model. *J. Atmos. Sci., 40,* 91–106.